Available online at www.sciencedirect.com
SCIENCE DIRECT®
Journal of Sound and Vibration 291 (2006) 986–1003
JOURNAL OF SOUND AND VIBRATION
www.elsevier.com/locate/jsvi

On estimating frequency response function envelopes using the spectral element method and fuzzy sets

R.F. Nunes[a], A. Klimke[b,*], J.R.F. Arruda[a]

[a]*Department of Computational Mechanics, University of Campinas, C.P. 6122, 13083-080 Campinas, SP, Brazil*
[b]*Institute of Applied Analysis and Numerical Simulation, University of Stuttgart, Pfaffenwaldring 57, 70569 Stuttgart, Germany*

Received 11 November 2004; received in revised form 27 June 2005; accepted 5 July 2005
Available online 5 October 2005

Abstract

The influence of uncertain input data on response spectra of dynamic structures is considered. Traditionally, frequency response analyses are based on finite or boundary element models of the objective structure. In the case of the mid-frequency range problem, however, a very fine mesh is required to correctly approximate the frequency response. This is particularly problematic in uncertainty modeling where the computational effort is usually increased significantly by the need for multiple runs (e.g. when conducting a Monte Carlo analysis) to achieve reliable results.

In this paper, the spectral element method, combined with a fuzzy set-based uncertainty modeling approach, is presented as an appealing alternative, provided that the models are simple enough to yield a spectral element representation. To conduct the fuzzy analysis part, three different implementations of the extension principle of fuzzy arithmetic are applied and compared. The suitability of each method depends on the number of uncertain parameters, the problem characteristics, and the required accuracy of the results. The performance of the proposed approach is illustrated by two test problems, a simple coupled rod and a reinforced plate model. To verify the fuzzy-valued results, a Monte Carlo simulation has also been included.

*Corresponding author. Tel.: +49 711 685 5543; fax: +49 711 685 5507.
E-mail addresses: ronaldo.nunes@daimlerchrysler.com (R.F. Nunes), klimke@ians.uni-stuttgart.de (A. Klimke), arruda@fem.unicamp.br (J.R.F. Arruda).

0022-460X/$ - see front matter © 2005 Elsevier Ltd. All rights reserved.
doi:10.1016/j.jsv.2005.07.024

1. Introduction

In recent years, considerable research effort has been placed in studying the mid-frequency range problem of structural dynamics. Of great practical importance in this field is the simulation of the frequency response under uncertain parameters, which can provide important answers during the design stage of products that must meet stringent noise and vibration criteria (e.g. automotive parts).

Possible sources of uncertainty are manifold. For instance, geometrical and material inconsistencies of components as well as their interaction with an unpredictable environment could be taken into account [1]. Simplifying assumptions made in the development phase of the mathematical models could further increase the uncertainty of the results. Other typical examples are uncertain parameters obtained by parameter identification processes subjected to measurement errors. An effort to categorize sources of uncertainty in dynamic engineering problems was made by Manohar and Gupta [2], who propose the following four categories: physical or inherent uncertainties, model uncertainties, estimation errors, and human errors. Keese [3] summarizes that uncertainties can be caused either by intrinsic variability of physical quantities, such as irregularities in material properties caused by the manufacturing process or simply by lack of knowledge, which he calls epistemic uncertainty.

Three predominant approaches are available to describe and quantify uncertainty mathematically, namely probability theory, interval analysis, and possibility theory based on fuzzy sets. With probability theory, stochastic processes are used to model system behavior that is to some extent unpredictable. Resulting probabilities can be estimated from a sufficiently large sample of realizations (outcomes) of random variables and stochastic processes [4]. For probabilistic uncertainty modeling approaches with applications to structural dynamics, see e.g. Refs. [5–8] and the references therein. Interval analysis [9] provides the means to deal with imprecise data, and is extensively used in tolerance analysis. Here, imprecision refers to a lack of knowledge about the value of a parameter that is in turn expressed as a crisp tolerance interval. A main advantage of interval analysis is its capability to provide guaranteed bounds on the results for given interval-valued input data. This fact implies the important distinction of a result to be *possible* rather than probable. Fuzzy set-based methods emerged from the work of Zadeh [10]. They are especially well suited for dealing with forms of uncertainty that are inherently non-statistical in nature. Instead of producing single intervals as outputs, possibility theory based on fuzzy sets permits gradations of possibility.

The rest of the paper is organized as follows: in Section 2, a brief summary of the spectral element method (SEM) is presented. Section 3 reviews the basics of fuzzy set theory and discusses possible numerical implementations of fuzzy arithmetic. In Section 4, we describe the proposed procedure for computing frequency response function (FRF) envelopes via SEM subjected to fuzzy-valued input data. In Section 5, we present two tests problems. We apply all three fuzzy arithmetical methods of Section 3 to illustrate the advantages and disadvantages of each method.

2. Review of the spectral element method

The formulation of the SEM used here was proposed by Doyle [11] in the context of wave propagation problems. The method is a systematization of the mobility approach developed much

earlier [12]. It uses the exact solution matrices with transcendental functions in the frequency domain, solving the dynamic problems with Fourier-based techniques. The basic idea of SEM is to combine the advantages of analytical spectral analysis with the efficiency and organization of the Finite Element Method (FEM). The main advantage of SEM in comparison to FEM is the fact that the spectral element dynamic stiffness matrix is computed in the frequency domain, which allows the stiffness and the inertia of the distributed-parameter system to be described exactly. Thus, it is not necessary to refine the mesh as the wavelength becomes smaller. It can be shown that the SEM dynamic stiffness matrix corresponds to an infinite number of finite elements [11].

The SEM is formulated based on two types of elements, *two-noded* and *single-noded* (also called *throw-off*) elements. The latter are adopted when the member extends to infinity and is connected at a single point (or line). The major drawback of SEM is that the elements may only be assembled in one dimension, and that the solution along the orthogonal dimensions have to be found analytically, which is only possible for simple geometries. Doyle proposes a more general approach [11], which consists of using image sources—fictitious forces are used to impose the desired boundary conditions, such as mirror sources in acoustics to model a rigid surface—but the approach still requires an ad hoc solution, which does not always exist. Thus, in the present stage, the spectral element formulation is applicable just for structural elements with simple geometry and boundary conditions [13,14].

In order to illustrate the proposed approach for including parametric uncertainty in SEM models, we describe the low-order spectral rod element in the following. This model is used for the first numerical example of Section 5, a system of two coupled rods. For a detailed description of the more complex SEM model for reinforced plates, as used in the second numerical example, please refer to Refs. [13,15].

We start with the following equation of motion [11]:

$$\frac{\partial}{\partial x}\left[EA\,\frac{\partial u}{\partial x}\right] = \rho A\,\frac{\partial^2 u}{\partial t^2} - q, \tag{1}$$

where EA is the axial stiffness with the Young's modulus E and the cross-sectional area A, and ρA is the mass density per unit length of the rod. Now, the spectral analysis can be applied with a solution of the form

$$\hat{u}(x,\omega) = \mathbf{A}e^{-ik_L x} + \mathbf{B}e^{-ik_L(L-x)}, \tag{2}$$

where $\mathbf{A}$ and $\mathbf{B}$ are the amplitudes at each frequency. Finally, by applying boundary conditions to a uniform wave-guide, the following symmetric matrix can be obtained:

$$\begin{Bmatrix}\hat{F}_1\\ \hat{F}_2\end{Bmatrix} = \frac{EA}{L}\,\frac{ik_L L}{(1-e^{-i2k_L L})}\begin{bmatrix}1+e^{-i2k_L L} & -2e^{-ik_L L}\\ -2e^{-ik_L L} & 1+e^{-i2k_L L}\end{bmatrix}\begin{Bmatrix}\hat{u}_1\\ \hat{u}_2\end{Bmatrix} = [\hat{k_e}]\{\hat{u}\}, \tag{3}$$

where $\hat{k_e}$ is the complex dynamic stiffness matrix for the rod element, $\hat{F}$ is the complex amplitude of the applied nodal forces, $\hat{u}$ is the vector of the complex amplitudes of the nodal displacements, and k_L is the wavenumber, which is given by $k_L = \sqrt{\omega^2\rho/E}$ in case of the rod.

In order to account for structural damping, an internal loss factor η can be applied by using a complex Young's modulus $E(1+i\eta)$.

From the dynamic stiffness matrices of the elements $\hat{k}_e$, a global dynamic stiffness matrix, $\hat{K}$, is easily assembled by using the direct stiffness method. The solution is found by solving a linear system of equations of the type $\{\hat{F}\} = [\hat{K}]\{\hat{U}\}$, where $\{\hat{U}\}$ is the global displacement vector. The FRFs are the elements of the inverse of the global dynamic stiffness matrix as a function of frequency.

3. Fuzzy set-based uncertainty modeling

Traditionally, probability theory is used to deal with uncertain information. However, as Dubois and Prade pointed out, there are important characteristics of uncertainty that cannot be handled appropriately by the probability theory [16], mainly since its key concepts are based on principles of randomness, which is not necessarily the source of uncertainty. In this paper, fuzzy sets are used to represent the uncertain input data.

3.1. Basics of fuzzy set theory

In the following, we briefly review the concepts of fuzzy sets. For a more detailed discussion of the basics of fuzzy set theory, see, for instance, Refs. [17, pp. 9–35], [18, pp. 10–14], [19, pp. 14–57].

Let X be a space whose generic elements are denoted by x, and let $\mu_{\tilde{A}} : X \to M \subseteq [0,1]$ be a characteristic function that maps X to the membership space M. Then, a *fuzzy set* is uniquely defined by the following set of pairs:

$$\tilde{A} = \{(x, \mu_{\tilde{A}}(x)) \,|\, x \in X\}. \tag{4}$$

$\mu_{\tilde{A}}$ is called *membership function*. If $M = \{0,1\}$, $\tilde{A}$ is called non-fuzzy or *crisp*. If $\sup_{x\in X} \mu_{\tilde{A}} = 1$, then the fuzzy set $\tilde{A}$ is called *normal*. In the following, it is assumed that all fuzzy sets are normalized.

The definition of the support of a fuzzy set, the notion of α-cuts, and the convexity of fuzzy sets are important preliminaries to computing functions of fuzzy sets, and are therefore defined in the following.

The *support* of a fuzzy set $\tilde{A}$ is the crisp set of all $x \in X$, such that $\mu_{\tilde{A}} > 0$, i.e.

$$\mathrm{supp}(\tilde{A}) = \{x \,|\, \mu_{\tilde{A}}(x) > 0,\ x \in X\}. \tag{5}$$

Let $\tilde{A}$ be a fuzzy set with $\tilde{A} = \{(x, \mu_{\tilde{A}}(x)), x \in X\}$. Then, the crisp set A_α with

$$A_\alpha = \{x \,|\, \mu_{\tilde{A}}(x) \geqslant \alpha, x \in X,\ 0 < \alpha \leqslant 1\} \tag{6}$$

is called α-*cut* or α-*level set* of $\tilde{A}$. In case of bounded supports, we also define the 0-cut as the closed interval $A_0 = [\inf(\mathrm{supp}(\tilde{A})), \sup(\mathrm{supp}(\tilde{A}))]$. α-cuts are often called *intervals of confidence*, since in case of convex fuzzy sets, α-cuts are closed intervals associated with a gradation of possibility or confidence between $[0,1]$.

A fuzzy set $\tilde{A} = \{(x, \mu_{\tilde{A}}(x)), x \in X\}$ is *convex*, if for all $a, b, c \in X$ with $a \leqslant b \leqslant c$,

$$\mu_{\tilde{A}}(a) \leqslant \mu_{\tilde{A}}(b) \quad \text{or} \quad \mu_{\tilde{A}}(c) \leqslant \mu_{\tilde{A}}(b). \tag{7}$$

Alternatively, a fuzzy set is convex if all α-level sets are convex in the conventional set-theoretic sense, i.e. if all α-level sets are connected.

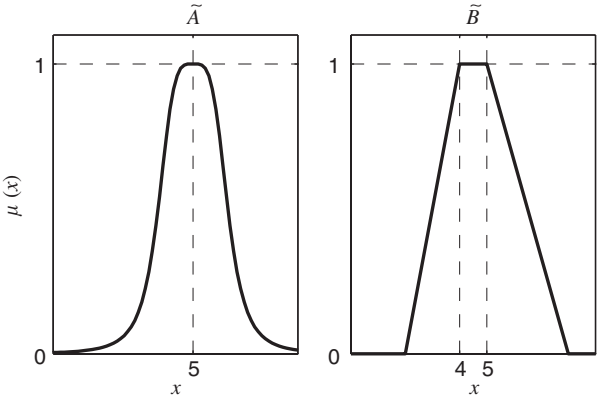

Fig. 1. Examples for convex fuzzy sets.

Example. Fig. 1 shows two examples for membership functions of convex fuzzy sets. The respective definitions of the fuzzy sets are

(1) $\tilde{A} = \{(x, \mu_{\tilde{A}}(x)) \mid \mu_{\tilde{A}}(x) = (1 + (x-5)^4)^{-1}, x \in \mathbb{R}\}$,
(2) $\tilde{B} = \{(x, \mu_{\tilde{B}}(x)) \mid x \in \mathbb{R}\}$, with

$$\mu_{\tilde{B}}(x) = \begin{cases} (x-2)/2 & \text{if } 2 \leqslant x < 4, \\ 1 & \text{if } 4 \leqslant x < 5, \\ (8-x)/3 & \text{if } 5 \leqslant x < 8, \\ 0 & \text{otherwise.} \end{cases}$$

We now proceed with the definition of Zadeh's extension principle [20]. It extends functions of real numbers to fuzzy-valued functions, and thus forms the theoretical basis of almost all methods for computing with fuzzy sets.

3.2. Extension principle

Let $\tilde{A}_1, \ldots, \tilde{A}_d$ be d fuzzy sets with the membership functions $\mu_1, \ldots, \mu_d$ defined on the spaces $X_1, \ldots, X_d$, respectively. Let $f : X_1 \times \cdots \times X_d \to Y$ be the objective function that maps the spaces $X_1 \times \cdots \times X_d$ to the space Y, i.e. $y = f(x_1, \ldots, x_d)$ and $y \in Y$. Then, the fuzzy image $\tilde{B}$ can be obtained by the formulae

$$\tilde{B} = \{(y, \mu_{\tilde{B}}(y)) \mid y = f(x_1, \ldots, x_d), (x_1, \ldots, x_d) \in X_1 \times \cdots \times X_d\}$$

with

$$\pi(x_1, \ldots, x_d) = \min(\mu_1(x_1), \ldots, \mu_d(x_d)),$$

$$\mu_{\tilde{B}}(y) = \begin{cases} \sup\limits_{y = f(x_1, \ldots, x_d)} (\pi(x_1, \ldots, x_d)) & \text{if } \exists y = f(x_1, \ldots, x_d), \\ 0 & \text{otherwise.} \end{cases} \tag{8}$$

If the fuzzy sets $\tilde{A}_1, \ldots, \tilde{A}_d$ of the extension principle are convex fuzzy sets with compact support, and the objective function $f : X_1 \times \cdots \times X_d \to Y$ is continuous, then the following *alternative formulation* is equivalent to Eq. (8) (for the proof see Ref. [21]).

$$\tilde{B} = \{(y, \mu_{\tilde{B}}(y)) \,|\, y \in Y\}$$

with

$$\mu_{\tilde{B}}(y) = \begin{cases} \sup\{\alpha \,|\, y \in B_\alpha\} & \text{if } y \in B_0, \\ 0 & \text{otherwise,} \end{cases}$$

$$B_\alpha = \left[\min_{\mathbf{x}\in\Omega_\alpha} f(\mathbf{x}), \max_{\mathbf{x}\in\Omega_\alpha} f(\mathbf{x})\right], \quad 0 \leqslant \alpha \leqslant 1. \tag{9}$$

In Eq. (9), $\Omega_\alpha = (A_1)_\alpha \times \cdots \times (A_d)_\alpha$, $0 \leqslant \alpha \leqslant 1$ denote the interval boxes formed by the α-cuts $(A_1)_\alpha, \ldots, (A_d)_\alpha$.

Usually, an implementation of the extension principle is based on the alternative formulation, which can be treated much easily by a numerical algorithm than the original formulation according to Zadeh, Eq. (8).

3.3. Implementation of the extension principle

We will use three different implementations of the extension principle, namely the reduced transformation method [22], the general transformation method [22], and the sparse grid approach [23]. In the following, a brief description of these methods is given. A common feature of all three methods is the fact that they require real-valued function evaluations only, they are thus directly applicable to a wide range of functions, including FEM models (see e.g. Refs. [24,25]) and SEM models for dynamic structures as in this paper. For a detailed discussion of the implementation of these methods, please refer to the provided references.

3.3.1. Reduced transformation method/FWA algorithm

The reduced transformation method [22] is an improved version of the classical FWA algorithm by Dong and Wong [26] that ensures convexity of the fuzzy result. It is based on the alternative formulation of the extension principle, Eq. (9). The first part of the method consists of discretizing the fuzzy-valued inputs into α-cuts. Permutations of the lower and upper bounds of the α-level sets are formed to obtain the corner points (''vertices'') of the d-dimensional boxes Ω_α in Eq. (9). If the objective function is monotonic with respect to all input parameters in the region Ω_0, these points suffice to correctly compute the resulting α-cuts. Otherwise, the method may underestimate the correct result.

The computational complexity is governed by the number of function evaluations N, which grow linearly with the number of considered α-cuts m and exponentially with the dimension d, i.e. $N = m2^d$.

3.3.2. General transformation method

The general transformation method proposed by Hanss [22] is an implementation of the extension principle that first discretizes the convex fuzzy sets into α-cuts, and then again discretizes

the α-cuts into sets of points. Due to the discretization scheme, only convex fuzzy sets $\tilde{A}$ with bounded support and a single value $\overline{m}$ with $\mu_{\tilde{A}}(\overline{m}) = 1$ may be used as inputs. The results of the transformation method can be made arbitrarily accurate by letting the number of α-cuts m go to infinity, but at the cost of a high computational complexity.

The cost of the general transformation method is governed by the number of function evaluations N. In this study, we use an efficient implementation of the general transformation method that eliminates recurring permutations [27]. In this case, with m denoting the number of α-cuts, N is given by $N = (m-1)^d + m^d$.

Note that the extended transformation method [28] cannot reduce the computational effort to less than $N = m^d$ function evaluations (even if monotonicity is detected), since it always requires to compute the 0-cut with a full grid. In case of non-monotonicity, the effort is significantly higher, i.e. $N = \sum_{k=1}^{m} m^d$. Therefore, we recommend to implement the general transformation method considering recurring permutations according to Ref. [27], as it has been done in this paper.

3.3.3. *Computing fuzzy functions using sparse grids*

The sparse grid method [23,29] is applicable to continuous functions, and the fuzzy input parameters must be convex with bounded support. The main idea of the method is to compute a sparse grid interpolant of the objective function with sufficient accuracy for the d-dimensional box Ω_0 in Eq. (9), using only a low number of real-valued function evaluations. The number of support nodes of the sparse grid interpolant grows only very moderately with increasing problem dimension d. The hierarchical structure of the sparse grid interpolation scheme permits to subsequently increase the interpolation depth until a sufficient estimated relative or absolute accuracy is reached. The interpolant then replaces the objective function in the optimization problems in Eq. (9). The subsequent optimization problems are solved by suitable global optimization algorithms that take advantage of the known properties of the interpolant.

The computational complexity of the sparse grid approach cannot be expressed as simply as for the other methods above, since it depends on the objective function itself. However, in case of expensive objective functions, the evaluation of the model at the support nodes of the interpolant usually governs the overall computation time. Depending on the type of the sparse grid used, the number of support nodes varies. Here, we have used the sparse grid with piecewise multilinear basis functions from Ref. [23], where the number of function evaluations N is at most

$$N \leqslant 2^{n+1} \cdot \frac{(n+d-1)!}{n!(d-1)!},$$

where n denotes the depth of the sparse grid, $n \in \mathbb{N}$. The interpolant can be made arbitrarily accurate with increasing n.

4. Estimating envelope FRFs using SEM and fuzzy sets

In this section, we describe the overall approach to computing envelope FRF magnitudes of dynamic structures using SEM and fuzzy sets. This proves to be very straightforward, since the fuzzy arithmetical methods described in the previous section allow us to keep the SEM model as it

is—only multiple real-valued evaluations of the model are required to obtain an approximate solution of the envelope. Thus, the method is applicable as easily as a Monte Carlo (MC) method, however, it is much more efficient as the numerical examples of the next section will illustrate.

Step 1: *Discretization*: First, the objective frequency range $[F_0, F_1]$ is divided into $s-1$ equidistant or logarithmically spaced steps, giving s discrete frequencies f_i, $i = 1, \ldots, s$. We suggest one to use a logarithmic distribution when analyzing the dynamic response especially in vibroacoustic applications, since in this case, the resonance frequencies usually lie close together with increasing frequency. It is advisable to compute the FRF for a crisp set of input parameters first to select an adequate resolution, i.e., capable of clearly resolving the resonance frequencies. The d uncertain input parameters $\tilde{p}_1, \ldots, \tilde{p}_d$ are discretized into N discrete parameter vectors $\mathbf{p}_j$, $j = 1, \ldots, N$, $\mathbf{p}_j \in \Omega_0$ according to the chosen implementation of the extension principle of Section 3, and Ω_0 as in Eq. (9). Note that in case of the reduced and the general transformation method, N is determined by the number of α-cuts m chosen for the fuzzy number discretization. The sparse grid approach requires the interpolation depth parameter n.

Step 2: *Model evaluation*: Then, the magnitude of the frequency response function $\mathrm{FRF}(f_i, \mathbf{p}_j)$ is computed for all $s \cdot N$ permutations. An efficient implementation may vectorize the calls to the SEM model to treat multiple discrete frequencies, or alternatively, several sets of parameter permutations at once.

Step 3: *FRF envelope construction*: In case of the reduced and general transformation methods, the resulting discrete frequency response magnitudes $\mathrm{FRF}(f_i, \mathbf{p}_j)$ can be used directly to compute an approximate envelope. For each α-cut $\in [0, 1]$ (where α must match the cuts selected for the discretization), we compute $\mathrm{FRF}_\alpha(f_i) = [\mathrm{FRF}_{\alpha,\min}(f_i), \mathrm{FRF}_{\alpha,\max}(f_i)]$, with

$$\mathrm{FRF}_{\alpha,\min}(f_i) = \min_{\mathbf{p}_j \in \Omega_\alpha} \mathrm{FRF}(f_i, \mathbf{p}_j) \tag{10}$$

and

$$\mathrm{FRF}_{\alpha,\max}(f_i) = \max_{\mathbf{p}_j \in \Omega_\alpha} \mathrm{FRF}(f_i, \mathbf{p}_j). \tag{11}$$

In case of sparse grid-based fuzzy arithmetic, the discrete frequency response magnitudes $\mathrm{FRF}(f_i, \mathbf{p}_j)$, $i = 1, \ldots, s$, $j = 1, \ldots, N$, are used to construct s sparse grid interpolants $A_{n+d,d}(\mathrm{FRF}(f_i))$ that approximate the FRF at each discrete frequency f_i in the parameter domain Ω_0. For a detailed description of constructing these sparse grid interpolants, see Refs. [23,29]. To obtain the frequency response envelope, a suitable global optimization algorithm [23] is used to compute

$$\mathrm{FRF}_{\alpha,\min}(f_i) = \min_{\mathbf{p} \in \Omega_\alpha} A_{n+d,d}(\mathrm{FRF}(f_i))(\mathbf{p}) \tag{12}$$

and

$$\mathrm{FRF}_{\alpha,\max}(f_i) = \max_{\mathbf{p} \in \Omega_\alpha} A_{n+d,d}(\mathrm{FRF}(f_i))(\mathbf{p}). \tag{13}$$

Here, any set of α levels can be chosen for the optimization part. Obviously, the sparse grid-based approach requires more computational effort to compute the envelope. However, often much fewer evaluations of the SEM model are required to compute an accurate approximation of the

response envelope. In case of complex, expensive to evaluate models, this can result in enormous time savings.

Remark. To obtain good results with the sparse grid-based approach, it is recommended to use FRF function values in *logarithmic* scale, i.e. use $\log(|\mathrm{FRF}(f_i, \mathbf{p}_j)|)$ to construct the interpolant, since the underlying multilinear interpolation scheme will produce more appropriate interpolated values.

Finally, the fuzzy-valued frequency response at any given frequency f_i can be composed from the α-level sets $\mathrm{FRF}(f_i)_\alpha$. Furthermore, the response function envelopes for a given interval of confidence α are easily obtained by plotting the two curves of the minimum and the maximum FRF magnitudes $\mathrm{FRF}_{\alpha,\min}(f_i)$ and $\mathrm{FRF}_{\alpha,\max}(f_i)$, respectively, over the frequencies $f_i \in [F_0, F_1]$.

5. Numerical applications

In this section, we provide numerical results for two test problems. Both models were subjected to two uncertain parameters.

To get a detailed insight into the performance of the SEM/fuzzy approach, we have performed several runs on the models with different discretization parameters. In all simulation runs, the frequency domain was decomposed into $s = 1000$ frequencies at logarithmically spaced steps. This resolution is much higher than it would have been necessary from a practical point of view to achieve good results. However, it permitted to visualize the subtle differences in the convergence behavior of the applied methods by zooming into the regions of interest.

We have also conducted an error analysis to assess the quality of the computed results. The reference solutions $R_{\min}$ and $R_{\max}$ at $\alpha = 0$ were obtained numerically with a highly accurate sparse grid interpolant using an interpolation depth of $n = 9$, which resulted in $N = 3329$ support nodes per frequency. The maximum error $e_{\max}$ and the average error $e_{\min}$ of the FRF envelopes were computed according to the following formulae:

$$e_{\max} = \max_{i=1,\ldots,s} [|\mathrm{FRF}_{0,\min}(f_i) - R_{\min}(f_i)| + |\mathrm{FRF}_{0,\max}(f_i) - R_{\max}(f_i)|], \tag{14}$$

$$e_{\mathrm{avg}} = \left[\sum_{i=1}^{s} [|\mathrm{FRF}_{0,\min}(f_i) - R_{\min}(f_i)| + |\mathrm{FRF}_{0,\max}(f_i) - R_{\max}(f_i)|]\right] \cdot s^{-1}. \tag{15}$$

For comparison, we have also included a MC simulation with $N = 10$, 100, and 1000 samples. The samples were uniformly distributed in Ω_0, generated by the pseudo-random number generator RAND of MATLAB.

5.1. Coupled rod system

In the first example, we consider a system of two coupled rods. An axial force P is applied to the free end of rod 1, as shown in Fig. 2. Table 1 summarizes the properties of rods 1 and 2 adopted for the numerical model. The free–free boundary condition was used. The modulus of elasticity $\tilde{E}$ and the damping loss factor $\tilde{\eta}$ are treated as uncertain parameters. Note that in this simulation,

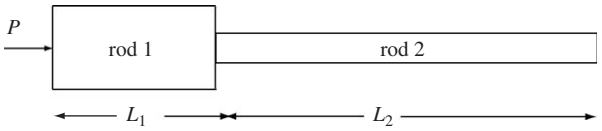

Fig. 2. Model of the coupled rod system.

Table 1
Physical and geometrical properties of the coupled rod system

Parameter	Mean value $\bar{m}$	Spread a	Unit
$\tilde{E}_{1/2}$	2.71×10^9	$10\%\bar{m}$	N/m^2
$\tilde{\eta}_{1/2}$	1.0×10^{-2}	$10\%\bar{m}$	—
$\rho_{1/2}$	1140	—	kg/m^3
A_1	1.735×10^{-3}	—	m^2
A_2	1.862×10^{-4}	—	m^2
L_1	0.20	—	m
L_2	2.46	—	m

$\tilde{E}_{1/2}$ and $\tilde{\eta}_{1/2}$ are not independent, i.e. $\tilde{E}_1 = \tilde{E}_2 = \tilde{E}$ and $\tilde{\eta}_1 = \tilde{\eta}_2 = \tilde{\eta}$, where $\tilde{E}$ and $\tilde{\eta}$ are the uncertain parameters. The uncertain parameters $\tilde{p}$ are modeled as triangular fuzzy numbers with spread a, i.e. $\tilde{p} = \langle \overline{m} - a, \overline{m}, \overline{m} + a \rangle$ according to the triplet notation of Kaufmann and Gupta [30]. We have studied the frequency response for the uncoupled case as well as the coupled case. For the coupled-rod case, the point receptance at the connection of the rods is considered (see Fig. 2).

One important feature of this setup is that rod 2 has a much higher modal density than rod 1, which implies that rod 2 acts as "fuzzy attachment" to rod 1 [31].

5.2. Plate with reinforcements

In the second example, a plate with simple supports in the yz-plane and free-free in the xz-plane is studied, see Fig. 3. Please also refer to Refs. [13,15] for a more detailed discussion of this model. Ref. [13] includes a review of the SEM formulation for reinforced plate elements and a comparison with a FEM approach. The assumed properties are summarized in Table 2. The FRF is computed at the drive point located at position $(x, y) = (333.4, 160.0)$ mm.

5.3. Simulation results

For the discretization parameters and the achieved accuracy of the runs, please refer to Table 3. The computed FRF envelopes including zooms for different discretization refinements are shown in Figs. 4–6, for the uncoupled rod, the coupled rod, and the plate system, respectively. Only the envelopes for the 0-cut are shown, which reflect the maximum variation for the considered uncertainty range. An exemplary fuzzy-valued result at a specific frequency f_k is shown in the

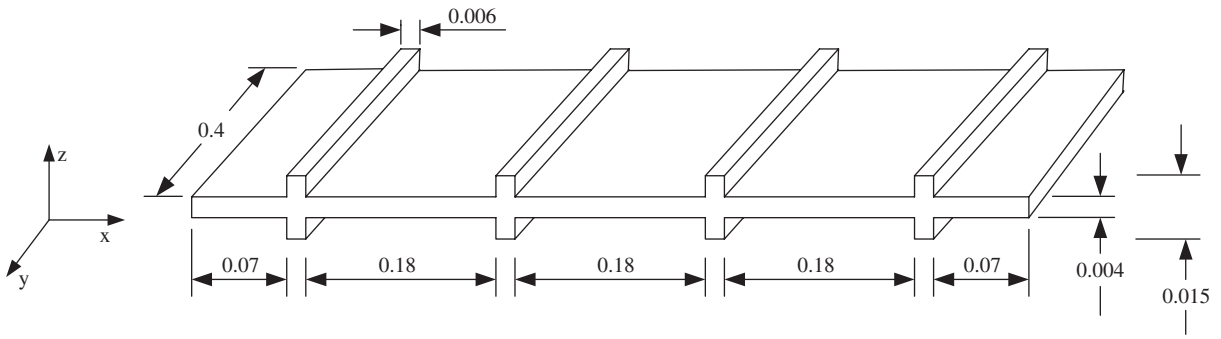

Fig. 3. Schematic diagram of the stiffened plate (units in meters) [13].

Table 2
Physical and geometrical properties of the plate

Parameter	Mean value $\bar{m}$	Spread a	Unit
$\tilde{E}$	69×10^9	$5\%\bar{m}$	N/m^2
$\tilde{h}$	4	$10\%\bar{m}$	mm
ρ	2700	—	kg/m^3
v	0.3	—	—
L_x	0.400	—	m
L_y	0.704	—	m

right-most column in case of the fuzzy-arithmetical methods (rtrm: reduced transformation method, gtrmrecur: general transformation method considering recurring permutations, sparse: sparse grid-based). For the MC analysis, the distribution of the sampled results at f_k is shown in the right-most column. The location of f_k in the frequency domain is indicated by the bold dashed line in the zoom plots.

5.4. Interpretation of the results

5.4.1. Accuracy

All of the deterministic fuzzy set-based methods significantly outperformed the MC analysis in terms of achieved accuracy vs. the number of required function evaluations. This is no surprise, since unlike in problems such as integration, where pure MC methods provide the attractive convergence order of $1/\sqrt{N}$ due to the central limit theorem independent of the problem dimension, the convergence order decreases exponentially with the dimension. We emphasize that the MC method was only used here to verify the correctness of the fuzzy-set-based results.

Both transformation method variants sample the corner points of the domain of the uncertain parameters, which are the relevant points when monotonicity is present. In proximity of the resonance frequencies, the response function is non-monotonic, and the sampled inner points become relevant. The reduced transformation method only samples the diagonals of the

Table 3
Discretization parameters and approximation error for the simulation runs

Method	m	n	N	Uncoupled rod		Coupled rod		Plate	
				e_{max}	e_{avg}	e_{max}	e_{avg}	e_{max}	e_{avg}
MC	—	—	10	4.6	1.3	7.4	0.57	14	3.3
	—	—	100	0.73	0.15	0.85	0.083	6.5	0.86
	—	—	1000	0.30	0.037	0.38	0.024	2.3	0.22
rtrm	2	—	5	5.0	0.52	7.0	0.37	14	3.0
	5	—	17	1.1	0.11	1.8	0.092	8.6	1.2
	17	—	65	0.49	0.054	0.58	0.042	3.9	0.33
	33	—	129	0.46	0.051	0.54	0.039	3.8	0.23
gtrmrecur	5	—	41	1.0	0.078	1.6	0.069	5.2	0.56
	17	—	545	0.085	0.0076	0.14	0.0068	0.55	0.059
	33	—	2113	0.028	0.0026	0.042	0.0023	—	—
sparse	21	1	5	5.0	0.56	7.2	0.39	15	3.0
	21	3	29	1.0	0.090	1.6	0.082	11	1.0
	21	5	145	0.096	0.0089	0.15	0.0080	5.2	0.27
	21	6	321	0.027	0.0023	0.036	0.0020	2.1	0.13

parameter domain hypercube, and is thus not guaranteed to converge to the correct result. This can be observed in the sub-plots (b,ii–iv) of the Figs. 4 and 5, where the envelope curve shows a kink near the peak, which is not present in the case of other methods (a,c,d,ii–iv).

The sparse grid-based approach showed mixed results. In the rod case, the performance was very good. Compared to the general transformation method, a significantly better asymptotic convergence rate was achieved (see Fig. 7), as was shown to hold in Ref. [23] for smooth functions. However, for the plate example, the encountered oscillations were too strong to be correctly resolved by an interpolant with a small number of nodes.

In summary, considering the error plot of Fig. 7, we suggest to use the reduced transformation method if only a crude approximation of the envelope is needed. For FRFs that do not exhibit a highly oscillatory behavior in the objective frequency domain, we suggest one to use sparse-grid-based approach. Otherwise, the general transformation method is most suitable.

5.4.2. *Performance*

In practice, it is of great importance to obtain simulation results quickly. We therefore give performance results of the discussed SEM/fuzzy approach in the following. All numerical tests were carried out using MATLAB V6.5 running on a Linux i686 1.6 GHz PC.

The evaluation of the coupled rod SEM model at 1000 discrete frequencies took $t_{rod} = 0.55$ s. The evaluation of the plate SEM model at 1000 discrete frequencies took $t_{plate} = 24$ s. The overhead of the transformation method variants was negligible in all runs (i.e., less than 0.1% of the overall computation time). The sparse grid-based approach required additional computing time depending on m and n; this took about $t_{sp} = 25-40$ s for the considered parameters $m = 21$ and $n = 1, \ldots, 5$. In the case of the plate model, this overhead was insignificant due to the

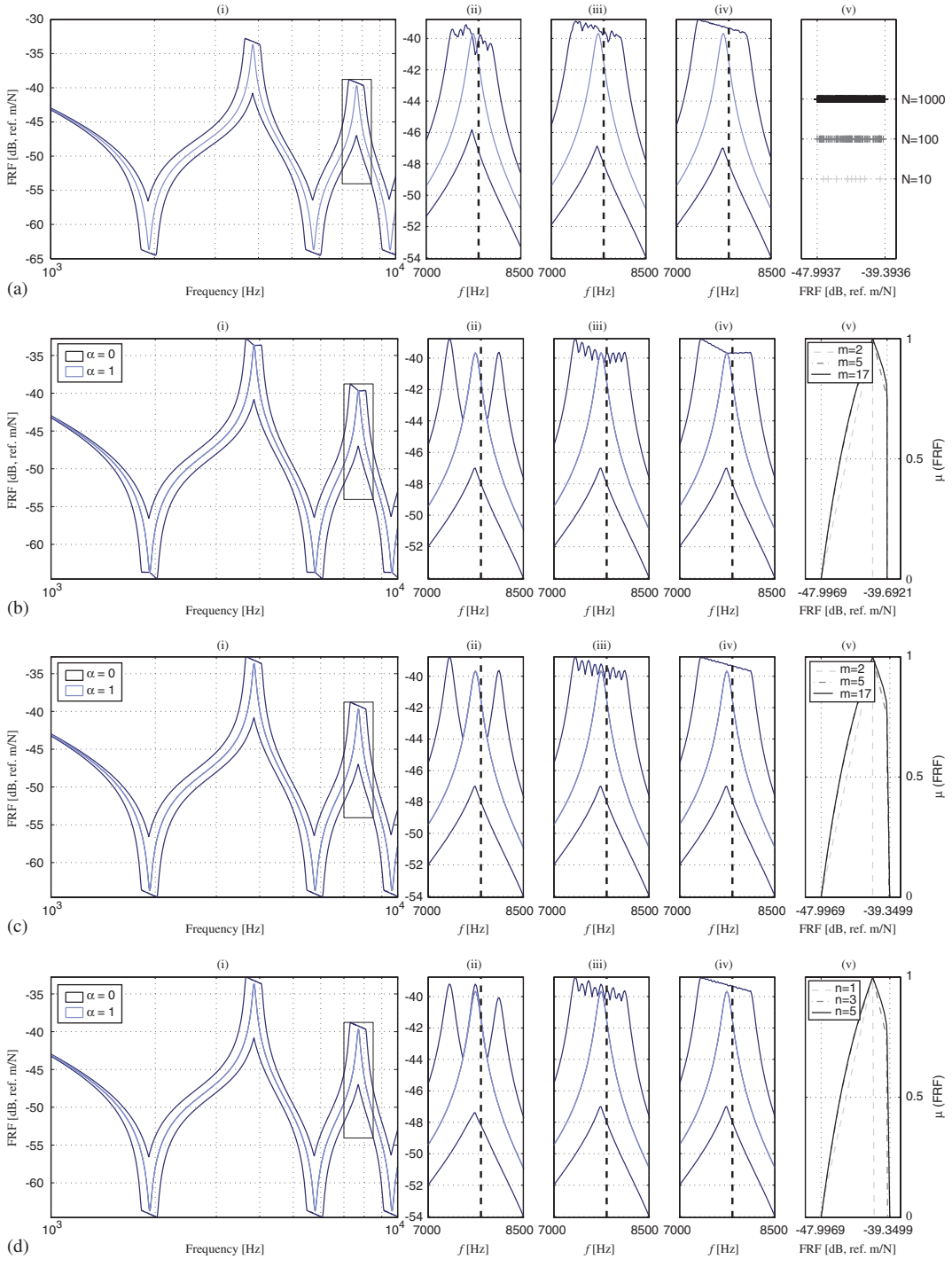

Fig. 4. Envelope FRFs for the uncoupled rod system: (a) MC, (b) rtrm, (c) gtrmrecur, (d) sparse grid; (i) full spectrum, (a,ii–iv) zoom for $N = 10, 100, 1000$, (b,c,ii–iv) zoom for $m = 2, 5, 17$ α-cuts, (d,ii–iv) zoom for level $n = 1, 3, 5$; (a,v) range of MC results depending on N at $f_{892} = 7796.4$ Hz, (b–d,v) fuzzy-valued result at f_{892} depending on m, n.

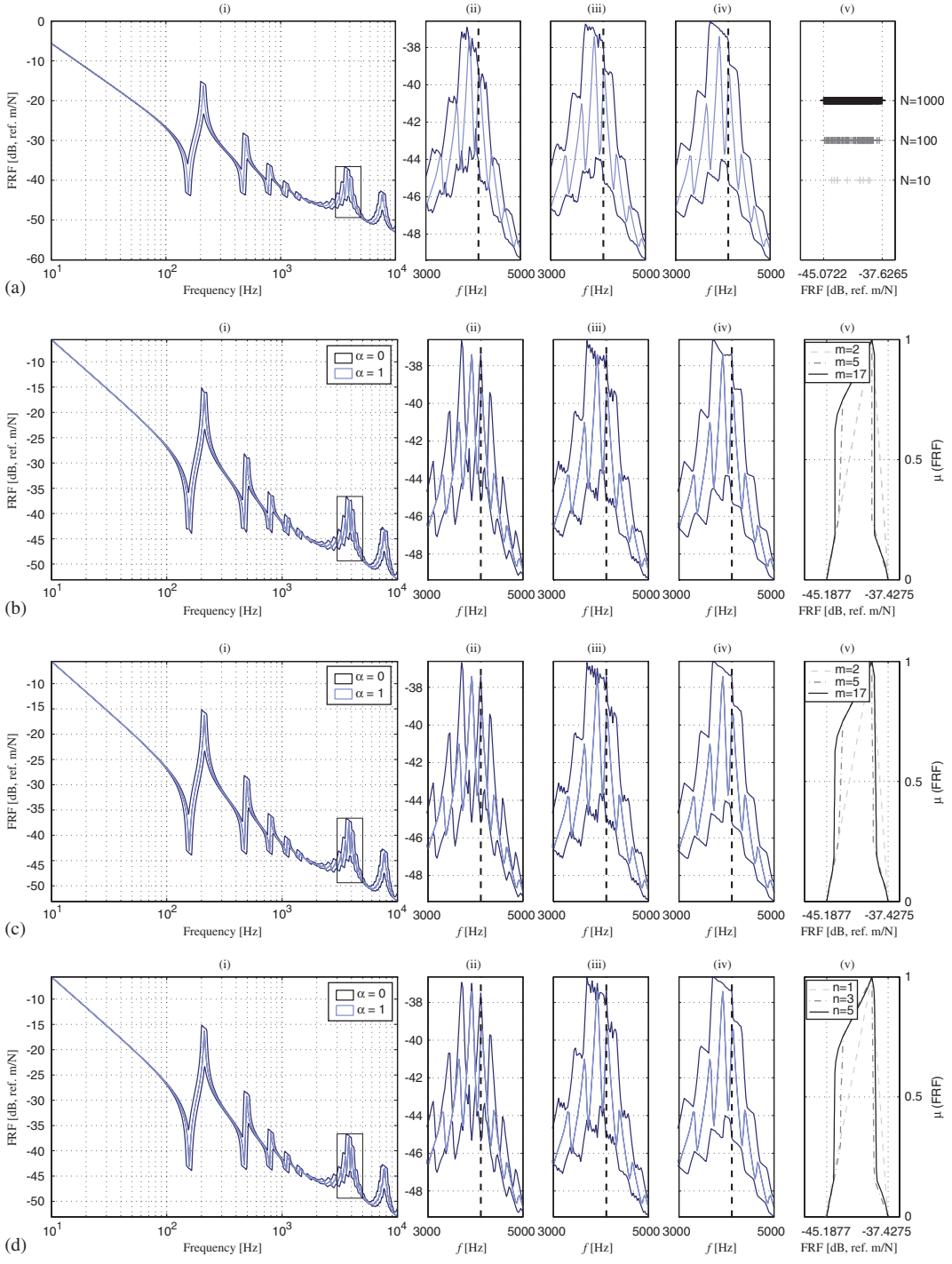

Fig. 5. Envelope FRFs for the coupled rod system: (a) MC, (b) rtrm, (c) gtrmrecur, (d) sparse grid; (i) full spectrum, (a,ii–iv) zoom for $N = 10, 100, 1000$, (b,c,ii–iv) zoom for $m = 2, 5, 17$ α-cuts, (d,ii–iv) zoom for level $n = 1, 3, 5$; (a,v) range of MC results depending on N at $f_{867} = 3986.6\,\text{Hz}$, (b–d,v) fuzzy-valued result at f_{867} depending on m, n.

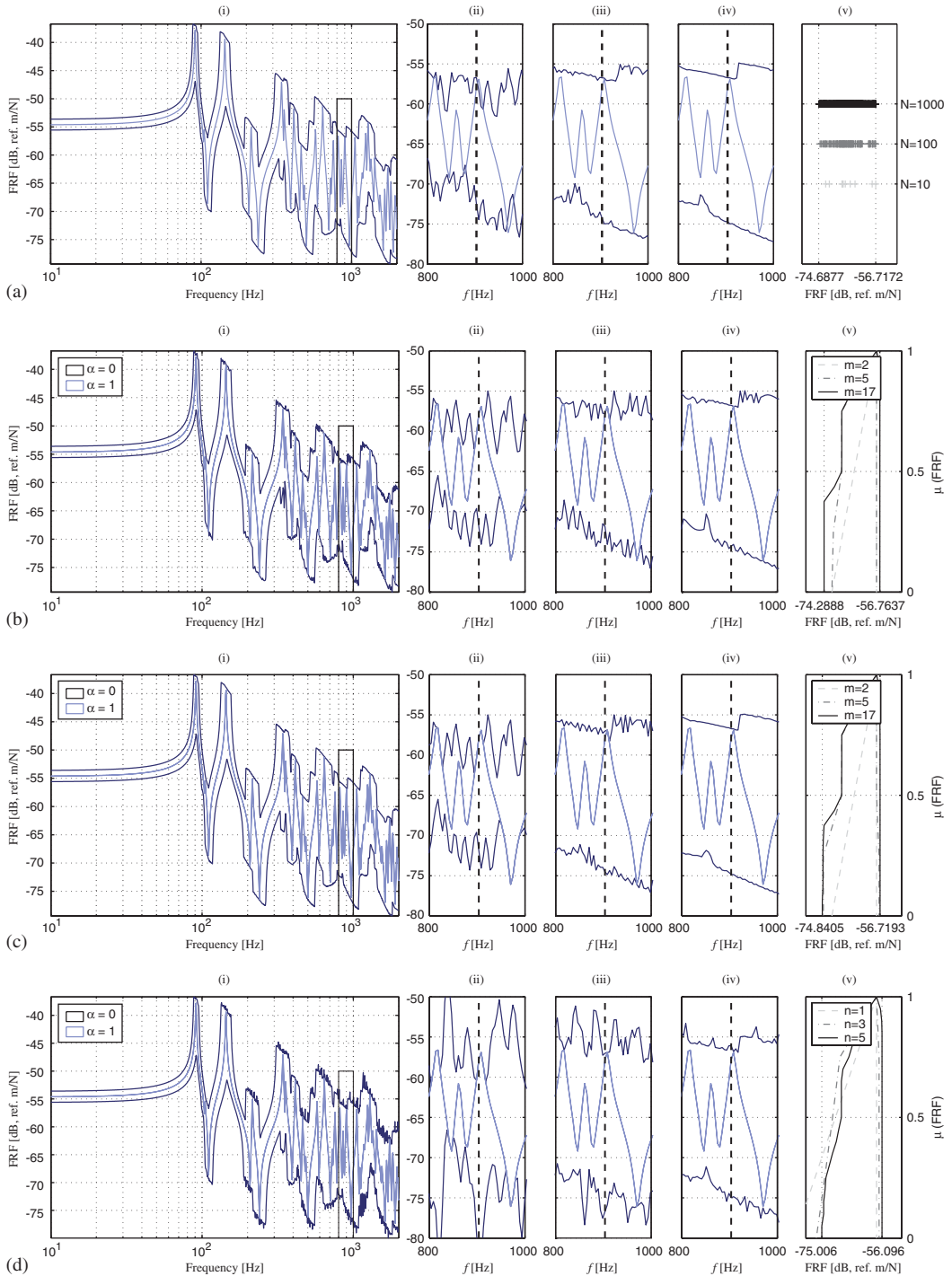

Fig. 6. Envelope FRFs for the plate system: (a) MC, (b) rtrm, (c) gtrmrecur, (d) sparse grid; (i) full spectrum, (a,ii–iv) zoom for $N = 10, 100, 1000$, (b,c,ii–iv) zoom for $m = 2, 5, 17$ α-cuts, (d,ii–iv) zoom for level $n = 1, 3, 5$; (a,v) range of MC results depending on N at $f_{849} = 897.90\,\text{Hz}$, (b–d,v) fuzzy-valued result at f_{849} depending on m, n.

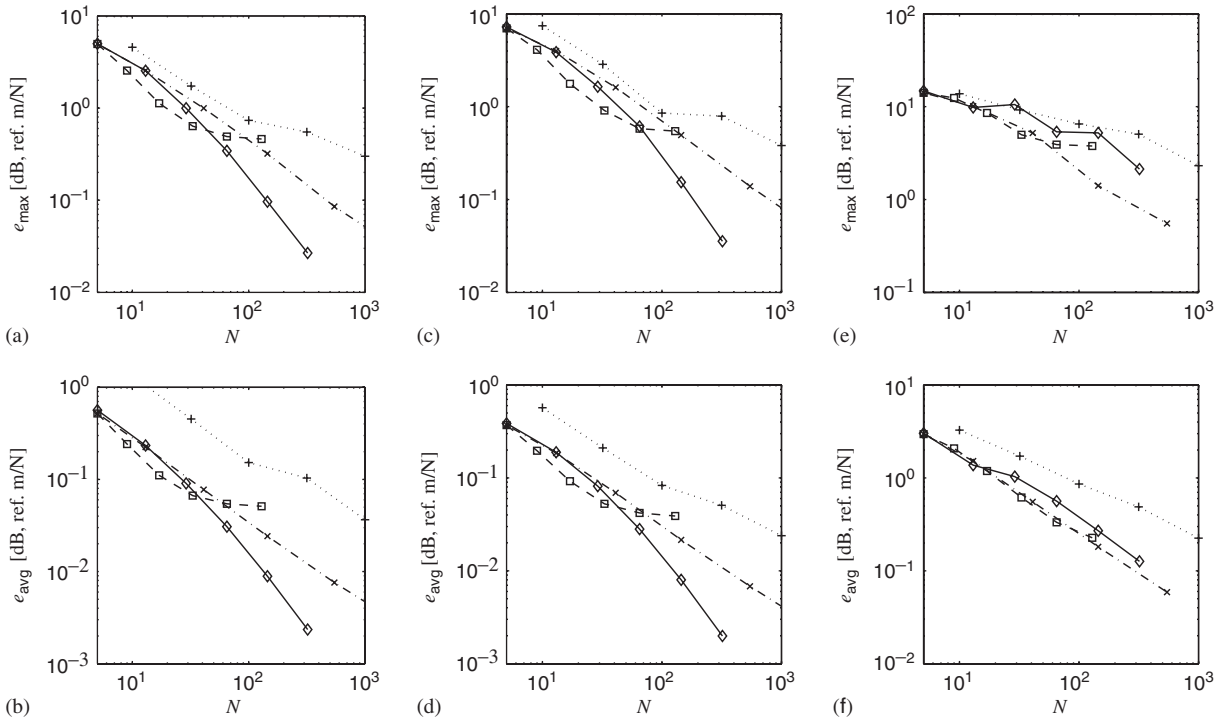

Fig. 7. Error plots: (a,b) uncoupled rod, (c,d) coupled rods, (e,f) plate; +: MC, ×: gtrmrecur, □: rtrm, ◇: sparse.

expensive model evaluations. The approximate overall run times can be obtained by multiplying t_{rod} and t_{plate} by N from Table 3, and adding t_{sp} in case of the sparse grid-based method.

5.4.3. Scalability

In this paper, only problems with two uncertain parameters were addressed. Let us assume that a maximum of about 1000 model evaluations per frequency is feasible in practice. The applicability of the reduced transformation is then limited to about $d = 8$ uncertain parameters if five α-cuts are used. The general transformation method scales significantly worse, since its complexity grows with $\mathcal{O}(m^d)$. Better results than with the reduced transformation method were only achieved for more than 10 α-cuts. Therefore, only models with up to three uncertain parameters are feasible. For $d = 4$, a sparse grid interpolant of level $n = 5$ requires 1105 function evaluations. For $d = 9$, a level 3 interpolant requires 1177 evaluations, which may still suffice depending on the smoothness of the FRF curve. Needless to say that a MC simulation would require significantly more than 1000 samples to produce reliable results in higher dimensions.

6. Conclusions

In this paper, the spectral element method was combined with fuzzy set methods to determine the frequency response function (FRF) envelopes for structures under uncertain input data. Three

different implementations of the extension principle of fuzzy arithmetic were applied and compared with a standard Monte Carlo analysis. The reduced transformation method is suggested to get an initial approximate solution with few function evaluations. If higher accuracies are required, and if the FRF curves are sufficiently smooth, such as the presented rod example, the sparse grid method performed best. In case of FRFs that exhibit a highly oscillatory response with very high local curvature, such as in the plate case, the general transformation method represented the most appropriate approach.

References

[1] S.M. Battil, J.E. Renaud, X. Gu, Modeling and simulation uncertainty in multidisciplinary design optimization, *AIAA* 4803 (2000) 1–11.
[2] C.S. Manohar, S. Gupta, Modeling and evaluation of structural reliability: current status and future directions, in: *Golden Jubilee Publications of Department of Civil Engineering, IISc-2002*, Bangalore, India, 2002, pp. 1–93.
[3] A. Keese, A review of recent developments in the numerical solution of stochastic partial differential equations (Stochastic Finite Elements), in: *Informatikbericht* No. 2003/06, Technical University Braunschweig, Braunschweig, Germany, 2003.
[4] H. Pradlwarter, G. Schuëller, Stochastic structural dynamics—a primer for practical applications, in: B.M. Ayyub (Ed.), *Uncertainty Modeling in Vibration and Fuzzy Analysis of Structural Systems, Series on Stability, Vibration and Control of Systems B*, vol. 10, World Scientific Publishing, Singapore, 1997, pp. 1–27 (Chapter 1).
[5] A. Sarkar, R. Ghanem, A substructure approach for the midfrequency vibration of stochastic systems, *Journal of the Acoustical Society of America* 113 (2003) 1922–1934.
[6] A. Sarkar, R. Ghanem, Mid-frequency structural dynamics with parameter uncertainty, *Computer Methods in Applied Mechanics and Engineering* 191 (2002) 5499–5513.
[7] C.S. Manohar, S. Adhikari, Dynamics stiffness of randomly parametered beams, *Probabilistic Engineering Mechanics* 13 (1998) 39–51.
[8] C.S. Manohar, S. Adhikari, Statistical analysis of vibration energy flow in randomly parametered trusses, *Journal of Sound and Vibration* 217 (1998) 43–74.
[9] L. Jaulin, M. Kieffer, O. Didrit, É. Walter, *Applied Interval Analysis*, Springer, London, Great Britain, 2001.
[10] L.A. Zadeh, Fuzzy sets, *Information and Control* 8 (1965) 338–353.
[11] J.F. Doyle, *Wave Propagation in Structures: Spectral Analysis Using Fast Discrete Fourier Transforms*, second ed., Springer, New York, 1997.
[12] W.H. Wittrick, F.W. Williams, A general algorithm for computing natural frequencies for elastic structures, *Quarterly Journal of Mechanics and Applied Mathematics* 24 (1971) 263–284.
[13] L. Donadon, E.L. Albuquerque, J.R.F. Arruda, Modeling reinforced plates using the spectral element method, in: *Proceedings of Inter-Noise*, Prague, Czech Republic, 2004.
[14] R.F. Nunes, S. Oexl, J.R.F. Arruda, Taking uncertainties into account in spectral element modeling of structures, in: *Proceedings of Inter-Noise*, Prague, Czech Republic, 2004.
[15] J.R.F. Arruda, L. Donadon, R.F. Nunes, E.L. Albuquerque, On the modeling of reinforced plates in the mid-frequency range, in: *Proceedings of ISMA-2004*, Leuven, Belgium, 2004.
[16] D. Dubois, H. Prade, *Possibility Theory*, Plenum Press, New York, 1988.
[17] D. Dubois, H. Prade, Fuzzy sets and systems, theory and applications, in: *Mathematics in Science and Engineering*, vol. 144, Academic Press, New York, 1980.
[18] H.-J. Zimmermann, Fuzzy sets, decision making, and expert systems, in: *International Series in Management Science/Operations Research*, Kluwer Academic Publishers, Boston, MA, 1987.
[19] H.-H. Bothe, *Fuzzy Logic*, second ed., Springer, Berlin, 1995.
[20] L.A. Zadeh, The concept of a linguistic variable and its application to approximate reasoning, *Information Science* 8 (1975) 199–249.
[21] J.J. Buckley, Y. Qu, On using α-cuts to evaluate fuzzy functions, *Fuzzy Sets and Systems* 38 (1990) 309–312.

[22] M. Hanss, The transformation method for the simulation and analysis of systems with uncertain parameters, *Fuzzy Sets and Systems* 130 (3) (2002) 277–289.
[23] A. Klimke, B. Wohlmuth, Computing expensive multivariate functions of fuzzy numbers using sparse grids, *Fuzzy Sets and Systems* 154 (3) (2005) 432–453.
[24] M. Hanss, *Applied Fuzzy Arithmetic*, Springer, Berlin, 2005.
[25] D. Moens, D. Vandepitte, Non-probabilistic approaches for non-deterministic dynamic FE analysis of imprecisely defined structures, in: *Proceedings of ISMA*, Leuven, Belgium, 2004.
[26] W.M. Dong, F.S. Wong, Fuzzy weighted averages and implementation of the extension principle, *Fuzzy Sets and Systems* 21 (1987) 183–199.
[27] A. Klimke, An efficient implementation of the transformation method of fuzzy arithmetic, in: E. Walker (Ed.), *Proceedings of NAFIPS-2003*, Chicago, IL, 2003, pp. 468–473.
[28] M. Hanss, The extended transformation method for the simulation and analysis of fuzzy-parameterized models, *International Journal of Uncertainty, Fuzziness and Knowledge-Based Systems* 11 (6) (2003) 711–727.
[29] A. Klimke, B. Wohlmuth, K. Willner, Uncertainty modeling using fuzzy arithmetic based on sparse grids: applications to dynamic systems, *International Journal of Uncertainty, Fuzziness and Knowledge-Based Systems* 12 (6) (2004) 745–759.
[30] A. Kaufmann, M.M. Gupta, *Introduction to Fuzzy Arithmetic*, Van Nostrand Reinhold, New York, 1991.
[31] R.S. Langley, P. Bremner, A hybrid method for the vibration analysis of complex structural-acoustic systems, *Journal of the Acoustical Society of America* 105 (1999) 1657–1671.